

UC Irvine

UC Irvine Previously Published Works

Title

The affinity of MhuD for heme is consistent with a heme degrading function in vivo†

Permalink

<https://escholarship.org/uc/item/0dh9d275>

Journal

Metallomics, 10(11)

ISSN

1756-5901

Authors

Thakuri, Biswash
Graves, Amanda B
Chao, Alex
et al.

Publication Date

2018-11-14

DOI

10.1039/c8mt00238j

Peer reviewed



Published in final edited form as:

Metallomics. 2018 November 14; 10(11): 1560–1563. doi:10.1039/c8mt00238j.

The affinity of MhuD for heme is consistent with a heme degrading function *in vivo*†

Biswash Thakuri^a, Amanda B. Graves^a, Alex Chao^b, Sommer L. Johansen^a, Celia W. Goulding^{b,c}, and Matthew D. Liptak^a

^aDepartment of Chemistry, University of Vermont, Burlington, Vermont 05405, USA

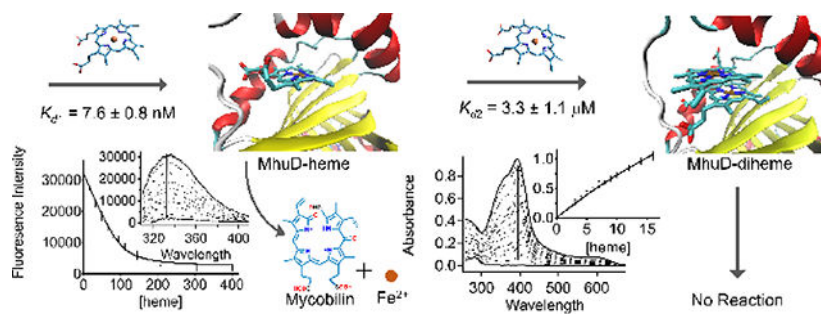
^bDepartments of Molecular Biology and Biochemistry, University of California-Irvine, Irvine, California 92627, USA

^cDepartment of Pharmaceutical Sciences, University of California-Irvine, Irvine, California 92627, USA

Abstract

MhuD is a protein found in mycobacteria that can bind up to two heme molecules per protein monomer and catalyze the degradation of heme to mycobilin *in vitro*. Here the K_{d1} for heme dissociation from heme-bound MhuD was determined to be 7.6 ± 0.8 nM and the K_{d2} for heme dissociation from diheme-bound MhuD was determined to be 3.3 ± 1.1 μ M. These data strongly suggest that MhuD is a competent heme oxygenase *in vivo*.

Graphical Abstract



TOC Figure. MhuD forms an enzymatically-active 1:1 complex with heme at nanomolar concentrations of labile heme and an inactive 1:2 complex at micromolar concentrations.

Mycobacterial infections are responsible for a range of human diseases, including two ancient ones: tuberculosis (*Mycobacterium tuberculosis* infection)¹ and leprosy (*Mycobacterium leprae* infection).² This genus has a unique heme acquisition pathway that is at least partially responsible for supplying a critical nutrient during infection by harvesting

†Electronic Supplementary Information (ESI) available: Experimental section, including derivation of eqn (1) and eqn (2), titration data for C-terminal His-tagged MhuD, further analysis of the UV/Vis Abs data, MhuD fractionation *in vitro* as a function of [heme], FPLC chromatographs, SDS-PAGE gels, DNA sequencing data, and ESI-MS data. See DOI: [10.1039/x0xx00000x](https://doi.org/10.1039/x0xx00000x)

matthew.liptak@uvm.edu.

iron from hemoglobin and perhaps other host heme-containing proteins.^{3, 4} Since bacteria require micromolar iron for growth,⁵ and the proteins of this pathway are unique to mycobacteria, the proteins of the mycobacterial heme acquisition system are promising drug targets.^{6, 7} Currently, this heme iron acquisition pathway is thought to begin with Rv0203, a secreted heme binding protein that could transport extracellular heme to the mycobacterial cell surface.⁸ Next, heme is transferred from Rv0203 to the periplasmic domains of inner membrane proteins MmpL3 or MmpL11.⁹ Finally, heme is degraded to non-heme iron and mycobilin by cytosolic MhuD.^{10–12} However, the precise mechanism of mycobacterial heme acquisition and the identities of the protein components are still poorly understood. In this communication, the details of heme binding by the putative terminal enzyme of the pathway, MhuD, will be addressed.

MhuD is a non-canonical heme oxygenase that catalyzes the monooxygenation of heme to meso-hydroxyheme, followed by dioxygenation of this intermediate to the mycobilin product.^{11, 13} This enzyme is unique among heme oxygenases in the fact that it can bind two heme molecules per protein monomer,¹⁰ and the di-heme-bound MhuD (MhuD–di-heme) form of the enzyme does not degrade heme. However, the heme dissociation constant for heme-bound MhuD (MhuD–heme) has been reported to be in the micromolar range,¹⁰ which is inconsistent with the nanomolar values reported for four other heme oxygenases: HO-1,¹⁴ HO-2,¹⁵ IsdG,¹⁶ and IsdI.¹⁶ Furthermore, the reported heme dissociation constant for MhuD–di-heme is also micromolar,¹⁰ implying that there is only a narrow labile heme concentration range where the enzymatically-active MhuD–heme form species can be formed. These observations call into question whether MhuD is a competent heme oxygenase *in vivo*, but a recent reinvestigation of the heme dissociation constants for *Staphylococcus aureus* IsdG and IsdI calls into question the accuracy of heme dissociation constants measured using micromolar protein samples.¹⁶ Thus, a reinvestigation of the MhuD–heme and MhuD–di-heme dissociation constants previously measured using isothermal titration calorimetry (ITC) and micromolar protein samples with a more sensitive spectroscopic technique is warranted in order to determine whether MhuD is a competent heme oxygenase *in vivo*.

The heme dissociation constants for MhuD–heme (K_{d1}) and MhuD–di-heme (K_{d2}) were measured using fluorescence and UV/Vis absorption (Abs) spectroscopy-based assays. A recombinant form of MhuD (*Rv3592*) with a C-terminal His₆ tag was expressed in and purified from *Escherichia coli* as previously described.^{10, 17} The K_{d1} for MhuD–heme and its standard error were determined using a previously described fluorescence assay that relies upon Förster resonance energy transfer (FRET) from Trp66 to enzyme-bound heme.¹⁶ Next, K_{d2} and its standard error was measured for MhuD–di-heme using Abs spectroscopy and a mathematical model derived in the ESI. Critical analyses of these data suggested that the C-terminal His₆ tag interferes with heme binding despite the fact that no interaction between heme and the His₆ tag was observed in the X-ray crystal structures of MhuD–heme or MhuD–di-heme.^{10, 17} For this reason, a form of MhuD with an enterokinase-cleavable N-terminal His₆-tag (MhuD_{CH}) was prepared. Measurements of K_{d1} and K_{d2} for MhuD_{CH} using fluorescence and Abs spectroscopies provide important insights into the interactions between MhuD and heme.

Fluorescence spectroscopy was used to measure K_{d1} for heme dissociation from MhuD–heme. This was accomplished using an assay originally developed for heme-bound *S. aureus* IsdG (IsdG–heme) and IsdI (IsdI–heme),¹⁶ which can also be used for MhuD–heme because a conserved tryptophan is located within 4 Å of the heme substrate for all three non-canonical heme oxygenases.^{17, 18} For MhuD, which can sequentially bind two heme substrates,¹⁰ the K_d value extracted from this experiment will correspond to K_{d1} because Trp66 fluorescence will be fully quenched by FRET to the first heme molecule bound by the active site. The fluorescence-detected titrations of heme into 100 nM MhuD yielded a K_{d1} of 4.2 ± 1.4 nM with an R^2 value of 0.908 (Fig. S1, ESI†). In comparison, analysis of the fluorescence-detected titrations of heme into MhuD_{CH} resulted in a K_{d1} of 7.6 ± 0.8 nM with an R^2 of 0.985 (Fig. 1). Thus, the K_{d1} values for heme dissociation from MhuD–heme and MhuD_{CH}–heme are similar, suggesting that the His₆ tag of MhuD minimally interferes with formation of the MhuD–heme complex. These K_{d1} values are three orders of magnitude lower than the value previously reported for MhuD–heme based upon ITC,¹⁰ but similar to those previously reported two other non-canonical heme oxygenases.¹⁶ Nevertheless, since there has been an issue in the literature with the accuracy of K_d values extracted from heme titrations into heme oxygenases,^{16, 19} the accuracy of the fit was further assessed.

In order to assess the goodness of fit, simulated titration curves for K_{d1} values one order of magnitude smaller and larger than the best fit were compared to the experimental data for MhuD_{CH}–heme (Fig. 2). Decreasing the K_{d1} value from the best fit of 7.6 nM to 0.76 nM lowered R^2 from 0.985 to 0.911 and resulted in a simulated titration curve that misses the error bars for six data points. Increasing K_{d1} to 76 nM decreased R^2 to 0.398 and produced a simulated curve that missed all but one of the experimental error bars. Thus, these data indicate that the nanomolar value measured here for K_{d1} is accurate, and the micromolar value measured previously is actually an upper limit due to the micromolar protein concentration required for ITC.¹⁰ Based upon the data presented in this manuscript, and that reported previously for IsdG–heme and IsdI–heme,¹⁶ it is reasonable to conclude that the K_d for heme dissociation from non-canonical heme oxygenases is nanomolar.

Following measurement of K_{d1} for MhuD–heme using fluorescence spectroscopy, Abs spectroscopy was used to measure K_{d2} for MhuD–diheme. Abs-detected titrations of heme into 5 μM MhuD or 5 μM MhuD_{CH} were monitored at 410 and 395 nm, respectively, and fit to eqn (2), which has been derived here as an analytical expression for sequential binding of two substrates to a single protein. These fits yielded K_{d2} values of 4.4 ± 7.2 nM and 3.3 ± 1.1 μM for MhuD–diheme and MhuD_{CH}–diheme, respectively (Figs. S2, ESI†, and 3). The value measured here for MhuD_{CH}–diheme is similar to the micromolar value reported previously based upon ITC,¹⁰ but three orders of magnitude higher than that reported here for MhuD–diheme. Careful inspections of the fits to eqn (2) reveal that the best fit line falls outside the experimental error bars for MhuD–diheme. Furthermore, the Soret band of MhuD_{CH} initially blue-shifts by 6 nm to 401 nm upon addition of up to two equivalents of heme, then red-shifts to 401 nm upon addition of a third equivalent of heme (Table S1,

†Electronic Supplementary Information (ESI) available: Experimental section, including derivation of eqn (1) and eqn (2), titration data for C-terminal His-tagged MhuD, further analysis of the UV/Vis Abs data, MhuD fractionation *in vitro* as a function of [heme], FPLC chromatographs, SDS-PAGE gels, DNA sequencing data, and ESI-MS data. See DOI: [10.1039/x0xx00000x](https://doi.org/10.1039/x0xx00000x)

ESI[†]). On the other hand, the Soret band of MhuD steadily blue-shifts from 408 nm to 394 nm upon addition of up to three equivalents of heme (Table S2, ESI[†]), suggesting that there is an additional interaction between MhuD and heme in the C-terminal His₆ tagged construct. The discrepancies between the two K_{d2} values reported in this work, and the one reported in the literature, motivated a careful assessment of the accuracy of the value reported here for MhuD_{CH}-diheme.

Similar to the strategy described above to assess the accuracy of the fluorescence analysis, the Abs data was compared to simulated titration curves for K_{d2} values one order of magnitude smaller and larger than the best fit (Fig. 4). The R² value for the fit decreased from 0.985 to 0.975 and 0.969 when titration curves were simulated for K_{d2} values of 0.33 and 33 μM, respectively. Furthermore, the best fit titration curve passes through all experimental error bars for MhuD_{CH}-diheme, whereas the fits for K_{d2} values one order of magnitude smaller or larger than the best fit do not. These analyses strongly suggest that the K_{d2} value reported here for MhuD_{CH}-diheme is accurate, and the His₆ tag interferes with measurement of this value. Since no interaction between the His₆ tag and the active site of MhuD was observed in the X-ray crystal structure of this species,¹⁰ the interference may be a weak interaction between the His₆ tag and labile heme. The fact that the K_{d2} value reported previously for MhuD-diheme based upon ITC is consistent with the accurate K_{d2} value reported here for MhuD_{CH}-diheme suggests that the interaction between the His₆ tag and the heme substrate has a minimal impact on the thermodynamics of heme binding. In summary, the data presented here indicate that K_{d1} for heme dissociation from MhuD_{CH}-heme is 7.6 ± 0.8 nM and K_{d2} for heme dissociation from MhuD_{CH}-diheme is 3.3 ± 1.1 μM.

Thus, the data presented here strongly suggest that MhuD is a competent heme oxygenase *in vivo*. The nanomolar K_{d1} for MhuD-heme is on the same order of magnitude as those previously reported for the heme-bound forms for other heme oxygenases,^{14–16} but the relevance of the K_{d1} values can perhaps be best understood by considering several scenarios. At sub-nanomolar concentrations of labile heme, the measured K_{d1} values imply that MhuD-heme and MhuD-diheme complexes are not stable and will dissociate prior to enzymatic turnover (Figure S3, ESI[†]), which means that any excess heme biosynthesis or acquisition relative to heme protein loading will increase the labile heme concentration.^{3, 4, 20} Once nanomolar concentrations of labile heme are reached, a stable MhuD-heme complex will be formed resulting in heme degradation and a reduction of the heme concentration by one molecule per turnover.^{10, 11} In a sense, this means that MhuD can buffer the labile heme concentration at a nanomolar level within *M. tuberculosis*. Two recent studies have established that the concentration of the cytosolic labile heme pool in *Homo sapiens* and *Saccharomyces cerevisiae* is 20–40 nM,^{21, 22} and notably in human IMR90 lung fibroblasts and HEK293 cells the labile heme pool is 400–600 nM,²³ so a nanomolar concentration of labile heme within *M. tuberculosis* is conceivable implying that MhuD-heme is a competent heme oxygenase *in vivo*. Despite the buffering capability of MhuD, it is conceivable that the labile heme concentration within *M. tuberculosis* could increase to micromolar levels if an inadequate amount of MhuD is present to buffer heme and/or if there is a high flux of heme into the organism via the heme acquisition system resulting in formation of a stable MhuD-diheme complex.

The biological function of MhuD–diheme is currently unknown, but here we speculate that MhuD may have a secondary function in its diheme form as a heme storage or heme sensor/regulatory protein. The diheme form of MhuD is unique among heme oxygenases and is one feature that distinguishes the MhuD enzyme found throughout mycobacteria from the IsdG enzymes found in Gram-positive bacteria and eukaryotic green algae.^{10, 19, 24–28}

Mycobacteria are a diverse genus that encounter a wide range of heme replete and deplete conditions, and any one of these conditions may be the origin of the MhuD–diheme function. For example, *Mycobacterium haemophilum* can only utilize heme as its sole exogenous iron source and has no siderophore-dependent iron uptake mechanism;^{29, 30} this is also the case for *M. leprae*.³¹ It is compelling to speculate that these two mycobacterial strains utilize MhuD to harbor a second heme molecule as a storage mechanism when faced with an abundance of host heme. Over the 100 nM to 100 μ M labile heme concentration range a significant mixture of MhuD–heme and MhuD–diheme would be present, and the storage function may act to slow the rate of heme degradation in order to accommodate the rate of MhuD product utilization by downstream enzymes. Alternatively, the MhuD–diheme form may act as a sensor/regulator, as many bacterial heme uptake systems have been shown to be regulated. In fact, both the *Pseudomonas aeruginosa* and *S. aureus* heme uptake systems are regulated by their heme degrading proteins albeit through different mechanisms.^{32, 33} Thus, these observations suggest that MhuD may have a dual function throughout mycobacteria, heme degradation and, possibly, heme storage or regulation.

In conclusion, a comprehensive study of heme binding by *M. tuberculosis* MhuD has been completed. Following removal of the His₆-tag, it was determined that the K_{d1} for heme dissociation from MhuD–heme is 7.6 ± 0.8 nM using a previously described fluorescence-based assay.¹⁶ An Abs assay was developed here to measure K_{d2} for heme dissociation from MhuD–diheme, which was revealed to be 3.3 ± 1.1 μ M. The low nanomolar K_{d1} value for MhuD–heme, coupled with the *in vitro* function of MhuD,^{11, 13} establishes this protein as a competent heme oxygenase *in vivo*. Based upon the micromolar K_{d2} value for MhuD–diheme, we speculate that MhuD may have a secondary function as a heme storage or regulatory protein, but the biological function of MhuD–diheme remains an open question that merits further investigation.

Supplementary Material

Refer to Web version on PubMed Central for supplementary material.

Acknowledgments

M.D.L. thanks the National Institutes of Health (R01-GM114277) and the National Science Foundation (DMR-1506248) for financial support. C.W.G. thanks the National Institutes of Health for financial support (P01-AI095208), and A.C. thanks the National Science Foundation for predoctoral fellowship support (DGE-1321846).

References

1. Lawn SD and Zumla AI, Lancet, 2011, 378, 57–72. [PubMed: 21420161]
2. Suzuki K, Akama T, Kawashima A, Yoshihara A, Yotsu RR and Ishii N, J. Dermatol, 2012, 39, 121–129. [PubMed: 21973237]

3. Tullius MV, Harmston CA, Owens CP, Chim N, Morse RP, McMath LM, Iniguez A, Kimmey JM, Sawaya MR, Whitelegge JP, Horwitz MA and Goulding CW, *Proc. Natl. Acad. Sci*, 2011, 108, 5051–5056. [PubMed: 21383189]
4. Jones CM and Niederweis M, *J. Bacteriol*, 2011, 193, 1767–1770. [PubMed: 21296960]
5. Weinberg ED, *Microbiol. Rev*, 1978, 42, 45–66. [PubMed: 379572]
6. Owens CP, Chim N and Goulding CW, *Future Med. Chem*, 2013, 5, 1391–1403. [PubMed: 23919550]
7. McLean KJ and Munro AW, *Drug Discovery Today*, 2017, 22, 566–575. [PubMed: 27856345]
8. Owens CP, Du J, Dawson JH and Goulding CW, *Biochemistry*, 2012, 51, 1518–1531. [PubMed: 22283334]
9. Owens CP, Chim N, Graves AB, Harmston CA, Iniguez A, Contreras H, Liptak MD and Goulding CW, *J. Biol. Chem*, 2013, 288, 21714–21728. [PubMed: 23760277]
10. Chim N, Iniguez A, Nguyen TQ and Goulding CW, *J. Mol. Biol*, 2010, 395, 595–608. [PubMed: 19917297]
11. Nambu S, Matsui T, Goulding CW, Takahashi S and Ikeda-Saito M, *J. Biol. Chem*, 2013, 288, 10101–10109. [PubMed: 23420845]
12. Contreras H, Joens MS, McMath LM, Le VP, Tullius MV, Kimmey JM, Bionghi N, Horwitz MA, Fitzpatrick JAJ and Goulding CW, *J. Biol. Chem*, 2014, 289, 18279–18289. [PubMed: 24855650]
13. Matsui T, Nambu S, Goulding CW, Takahashi S, Fujii H and Ikeda-Saito M, *Proc. Natl. Acad. Sci*, 2016, 113, 3779–3784. [PubMed: 27006503]
14. Koga S, Yoshihara S, Bando H, Yamasaki K, Higashimoto Y, Noguchi M, Sueda S, Komatsu H and Sakamoto H, *Anal. Biochem*, 2013, 433, 2–9. [PubMed: 23068042]
15. Fleischhacker AS, Sharma A, Choi M, Spencer AM, Bagai I, Hoffman BM and Ragsdale SW, *Biochemistry*, 2015, 54, 2709–2718. [PubMed: 25853617]
16. Conger MA, Pokhrel D and Liptak MD, *Metallomics*, 2017, 9, 556–563. [PubMed: 28401968]
17. Graves AB, Morse RP, Chao A, Iniguez A, Goulding CW and Liptak MD, *Inorg. Chem*, 2014, 53, 5931–5940. [PubMed: 24901029]
18. Lee WC, Reniere ML, Skaar EP and Murphy MEP, *J. Biol. Chem*, 2008, 283, 30957–30963. [PubMed: 18713745]
19. Skaar EP, Gaspar AH and Schneewind O, *J. Biol. Chem*, 2004, 279, 436–443. [PubMed: 14570922]
20. Dailey HA, Gerdes S, Dailey TA, Burch JS and Phillips JD, *Proc. Natl. Acad. Sci*, 2015, 112, 2210–2215. [PubMed: 25646457]
21. Song Y, Yang M, Wegner SV, Zhao J, Zhu R, Wu Y, He C and Chen PR, *ACS Chem. Biol*, 2015, 10, 1610–1615. [PubMed: 25860383]
22. Hanna DA, Harvey RM, Martinez-Guzman O, Yuan X, Chandrasekharan B, Raju G, Outten FW, Hamza I and Reddi AR, *Proc. Natl. Acad. Sci*, 2016, 113, 7539–7544. [PubMed: 27247412]
23. Yuan X, Rietzschel N, Kwon H, Nuno ABW, Hanna DA, Phillips JD, Raven EL, Reddi AR and Hamza I, *Proc. Natl. Acad. Sci*, 2016, 113, E5144–E5152. [PubMed: 27528661]
24. Skaar EP, Gaspar AH and Schneewind O, *J. Bacteriol*, 2006, 188, 1071–1080. [PubMed: 16428411]
25. Puri S and O'Brian MR, *J. Bacteriol*, 2006, 188, 6476–6482. [PubMed: 16952937]
26. Haley KP, Janson EM, Heilbronner S, Foster TJ and Skaar EP, *J. Bacteriol*, 2011, 193, 4749–4757. [PubMed: 21764939]
27. Duong T, Park K, Kim T, Kang SW, Hahn MJ, Hwang H-Y and Kim KK, *Acta Crystallogr., Sect. D*, 2014, D70, 615–626. [PubMed: 24598731]
28. Lojek LJ, Farrand AJ, Wisecaver JH, Blaby-Haas CE, Michel BW, Merchant SS, Rokas A and Skaar EP, *mSphere*, 2017, 2, e00176–00117. [PubMed: 28815214]
29. Sompolinsky D, Lagziel A, Naveh D and Yankilevitz T, *Int. J. Syst. Bacteriol*, 1978, 28, 67–75.
30. Tufariello JM, Kerantzas CA, Vilchéze C, Calder RB, Nordberg EK, Fischer JA, Hartman TE, Yang E, Driscoll T, Cole LE, Sebra R, Maqbool SB, Wattam AR and Jacobs WR, *mBio*, 2015, 6, e01313–01315. [PubMed: 26578674]

31. Cole ST, Eglmeier K, Parkhill J, James KD, Thomson NR, Wheeler PR, Honoré N, Garnier T, Churcher C, Harris D, Mungall K, Basham D, Brown D, Chillingworth T, Connor R, Davies RM, Devlin K, Duthoy S, Feltwell T, Fraser A, Hamlin N, Holroyd S, Hornsby T, Jagels K, Lacroix C, Maclean J, Moule S, Murphy L, Oliver K, Quail MA, Rajandream M-A, Rutherford KM, Rutter S, Seeger K, Simon S, Simmonds M, Skelton J, Squares R, Squares S, Stevens K, Taylor K, Whitehead S, Woodward JR and Barrell BG, *Nature*, 2001, 409, 1007–1011. [PubMed: 11234002]
32. Mouriño S, Giardina BJ, Reyes-Caballero H and Wilks A, *J. Biol. Chem.*, 2016, 2016, 20503–20515.
33. Videira MAM, Lobo SAL, Silva LSO, Palmer DJ, Warren MJ, Prieto M, Coutinho A, Sousa FL, Fernandes F and Saraiva LM, *Mol. Microbiol.*, 2018, Accepted Article.

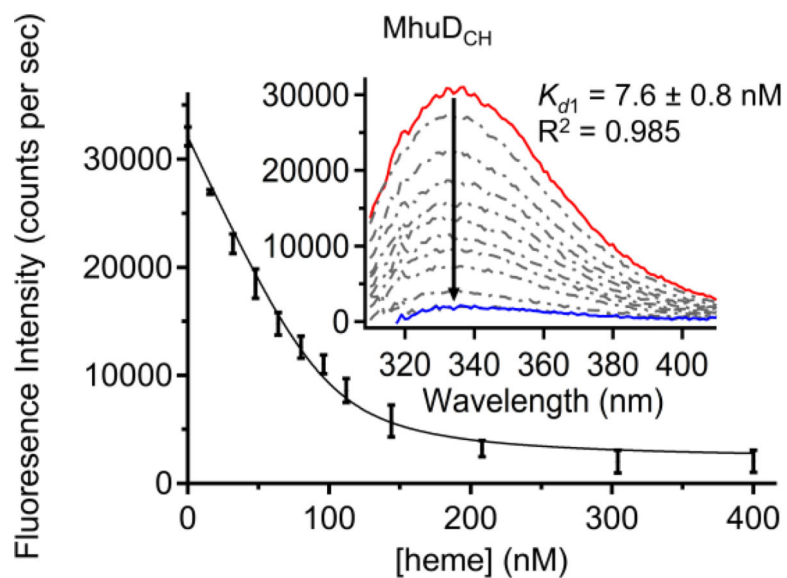


Fig. 1. Fluorescence-detected titration of heme into 100 nM MhuD_{CH} in 50 mM Tris pH 7.4, 150 mM NaCl. The error bars represent the standard deviation of three independent trials. The emission intensity was fit to equation (1) yielding a K_{d1} of 7.6 ± 0.8 nM. Inset: Emission spectra with 0 (solid red), 4 (solid blue), and intermediate (dashed gray) equivalents of heme.

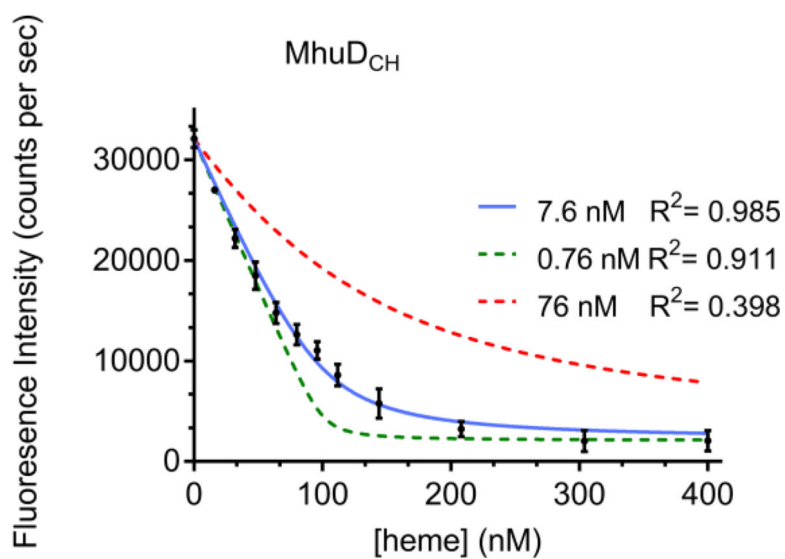


Fig. 2. Best fit of the fluorescence-detected heme titrations for MhuD_{CH} using equation (1) (solid blue). The error bars represent the standard deviation of three independent trials. Titration curves simulated using equation (1) and K_{dI} values one order of magnitude larger (dashed red) or smaller (dashed green) than the best fit are inconsistent with experiment.

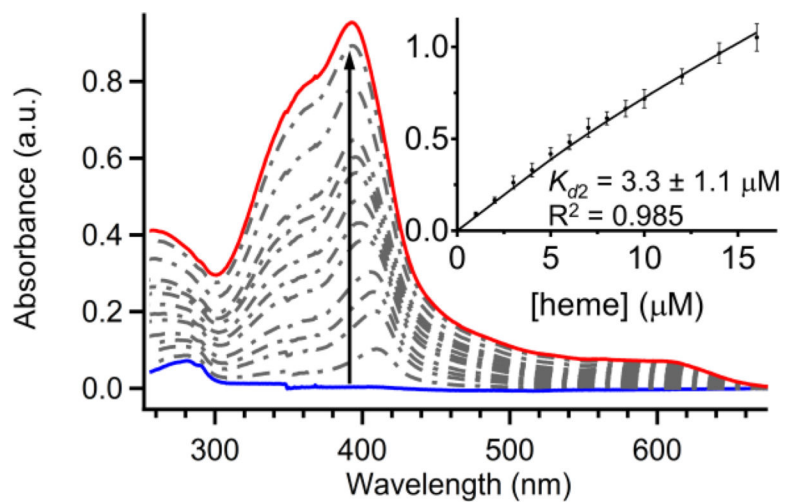


Fig. 3. Abs-detected titration of heme into 5 μM MhuD_{CH} in 50 mM Tris pH 7.4, 150 mM NaCl. The spectra represent MhuD_{CH} with 0 (solid blue), 3 (solid red), and intermediate (dashed gray) equivalents of heme. Inset: The error bars represent the standard deviation of three independent trials. The Abs-detected heme titration was fit to equation (2) yielding a K_{d2} of $3.3 \pm 1.1 \mu\text{M}$.

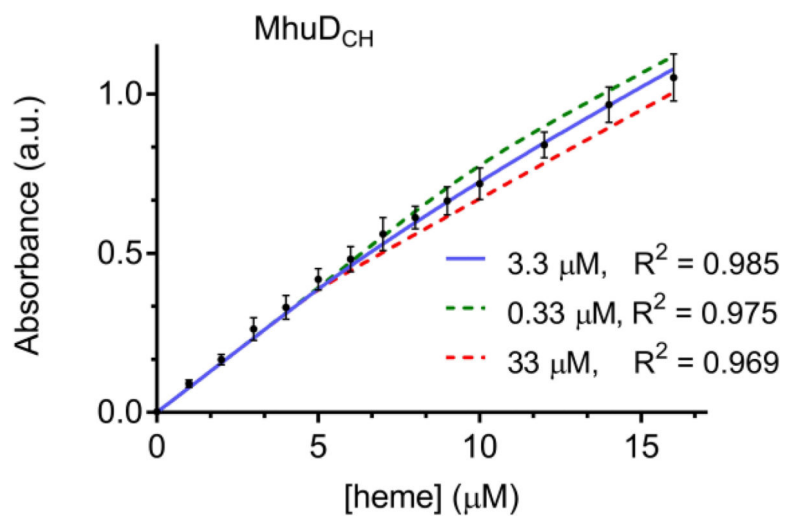


Fig. 4.

Best fit of the Abs-detected heme titrations for MhuD_{CH} using equation (2) (solid blue). The error bars represent the standard deviation of three independent trials. Titration curves simulated using equation (2) and K_{D2} values one order of magnitude larger (dashed red) or smaller (dashed green) than the best fit are inconsistent with experiment.